

# Funneling Study With A Low Energy Proton Beam\*

W. Barth, A. Schempp

Institut für Angewandte Physik, J.W. Goethe-Universität  
D-6000 Frankfurt 11, Postfach 111932, Germany

## Abstract

Funneling is a method to increase the brightness of ion beams by filling all rf-buckets in order to use the full current transport capability of an rf accelerator by frequency jumps at higher energies. This has been proposed for HIF type drivers and neutron sources.

A simple funneling experiment is prepared at Frankfurt, using modest fields in a set up with a 50 keV proton beam and an rf deflector to study especially emittance growth effects in such funneling lines. First results will be reported.

## I. INTRODUCTION

Funneling of two or more beams will drastically reduce the cost and complexity of accelerators designed to produce intense beams with brightness. Particle beams e.g. from two identical low-frequency structures are funneled into a single high frequency accelerator in such a way that every bucket of the high-frequency accelerating field is filled. For a simple two channel line the two beams have to be bunched and accelerated in identical rf accelerators at the frequency  $f_0$ , with a phase shift of 180 degrees between them (Fig. 1.).

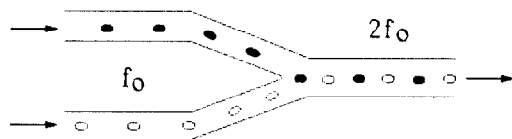


Fig. 1. Principle of a simple two channel funneling line.

A perfect funneling line doubles the beam current and the transverse brightness at twice the frequency without any emittance growth. Applications of funneling could include accelerators for heavy ion inertial fusion (HIF) or SNQ-type accelerators proposed for fusion material irradiation or accelerator production of tritium (APT) [1].

Funneling in a RFQ-like structure is a possibility for beam merging at low energies where electric fields are necessary to provide strong focusing. It has been shown that a single RFQ-like structure can be used to combine two ion beams [2].

For high energies funneling with discrete elements (quadrupoles, bending magnets, rebunchers,

rf deflectors) is more flexible but also more expensive. A first description of such a funnel line was given by Bongardt [3] for the HIBALL. Another funnel set up for HIBALL II has been proposed at LANL [4], where also a single leg of a prototype 5-MeV funnel for light ions was successfully tested [5].

## II. DEFUNNELING

Experimentally there are a lot of difficulties. Therefore we investigated funnel structures at first in a different way: one bunched ion beam is divided in two displaced beams with 180° phase-shift and half repetition frequency. A perfect defunnel line divides the beam current and the transverse brightness without any emittance growth. This inversion of a funnel line allows to investigate most of the physics issues, which arise in a real funnel section. For example the design and operating of the rf deflector - the neuralgic point of every funnel - can be optimized. Furthermore we can use the defunnel line itself as an injection system for a funnel experiment, because the two output beams of the defunnel line have all the required properties.

## III. FIELD CALCULATIONS

The deflector is a plate capacitor of length  $L$  symmetrically placed around the  $z$ -axis (the longitudinal axis of the injection accelerator) with a time varying electric field. If we neglect fringing fields at first, the electric field inside the deflector has only a homogenous and time-dependent  $x$ -component.

$$E_x(t) = A \sin(\omega t - \varphi) \quad (1)$$

Besides the peak deflecting amplitude  $A$ , such an ideal deflector is described by its length  $L$ , the frequency  $\omega$  and the phase  $\varphi$ .

Considering fringing fields ( $x$ -component),  $A$  is replaced by a term  $A(z)$ , which depends on  $z$ . Therefore, we used a version of the SLAC166 simulation code [6,7] to calculate the potential  $\Phi(x,z)$  in the deflector. From this the electric field component  $E_x(z)$  on axis is obtained.

In a next step the dependence of  $E_x$  on  $x$  and also the accelerating or decelerating field component  $E_z(x,z)$  is investigated. For that purpose we used the complete potential grid calculated by SLAC166 (see Fig. 2.). The actual field components

\* supported by BMFT under contract no. 06 OF186 I

are obtained by using the actual coordinates ( $x_{act}$ ,  $z_{act}$ ) of the particle (an example is shown in Fig. 3a and 3b.). This is done for every particle in the multiparticle simulations.

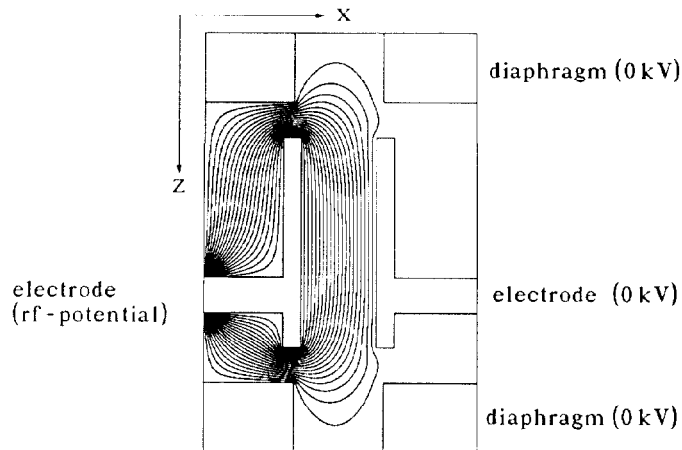


Fig. 2. The equipotential lines in the rf-deflector calculated with the SLAC166 [6,7].

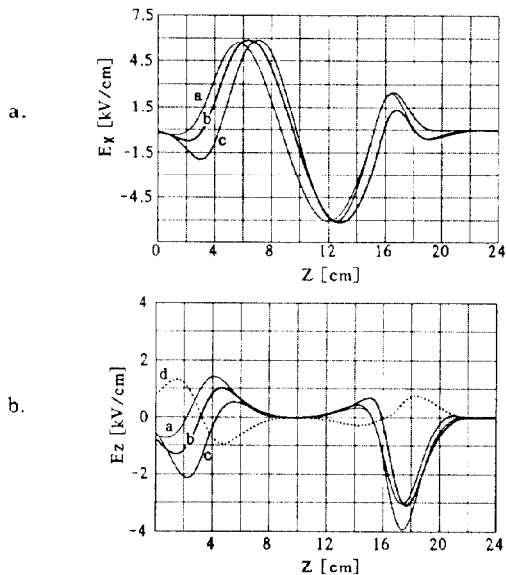


Fig. 3. a. The deflecting field component  $E_x(x,z)$ ;  $E_x$  for a particle at the beginning (c), at the end (a) and in the center (b) of the bunch is shown. b. The longitudinal field component  $E_z(x,z)$  (corresponds to Fig. 3a.); in addition  $E_z$  for a particle in the center of an adjacent bunch (d).

#### IV. EXPERIMENTAL SET UP

The experimental set up of the defunnel line is shown in Fig. 4. The injection system of the defunnel element consists of a plasma beam ion source [8], an extraction system, and a Split Coaxial-RFQ with rod electrodes [9].

With hydrogen operation the plasma beam ion source supplies a proton fraction of 90% at a max. beam current of 6 mA. The ions are extracted with an accel/decel-system at an extraction voltage of 6.5 keV. We use a solenoidal lens [10] to

match the ion source beam to the 50 MHz SCR-RFQ. The SCR-RFQ accelerates the  $H^+$ -beam from 6.5 keV to 50 keV.

In the adjacent defunnel element (25 MHz) the beam is divided into parallel beams. The deflector is part of a helix- $\lambda/4$ -resonator. Thus the cavity of the deflector can be very small.

For diagnostic we use faraday cups (beam current, bunchstructure), an emittance measurement device [11] and an analysing magnet for energy spectra. The parameters of the defunnel system are summarized in Tab. 1.

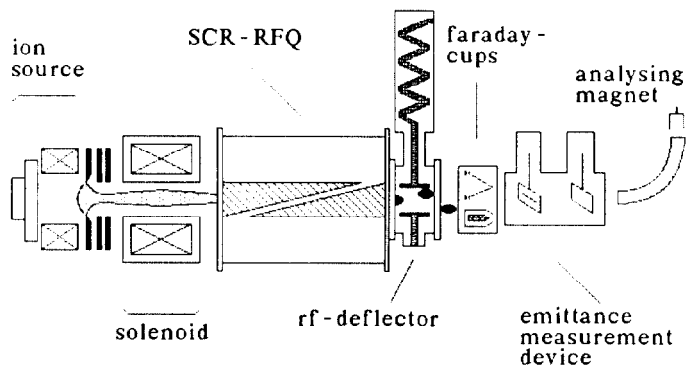


Fig. 4. The experimental set up of the defunnel line.

	SCR-RFQ	RF-Defl.
f (MHz)	50	25
Voltage (kV)	9	max. 40
Rp-value (k $\Omega$ )	180	290
Qo-value	4500	400
T <sub>in</sub> (keV)	6.5	50
T <sub>out</sub> (keV)	50	50
Aperture (mm)	6 - 4.5	42
Modulation	1.16 - 1.88	-
$\varphi_s$ ( $^\circ$ )	60 - 30	-
$\varphi_{ot}$ ( $^\circ$ )	45	-
Length (cm)	55	10 or 16
Cell number ( $\beta\lambda$ )	32	0.5 or 1
I <sub>max</sub> (mA)	4.2	-
Displacement (mm)	-	25

Tab. 1. The parameters of the defunnel experiment.

#### V. MULTIPARTICLE SIMULATIONS AND EXPERIMENTAL RESULTS

The horizontal beam deflection and the horizontal emittance growth were measured as a function of the relative rf-phase and the deflector voltage. Fig. 5. shows the horizontal beam deflection versus deflector voltage. The asymmetric field distribution - shown in Fig. 2. - is responsible for the differences between a deflection to the left or to the right side. The agreement between measurement and simulations is excellent. The beam deflection scales with deflection voltage as expected. The emittance growth (Fig. 6.) shows a dependence on the deflector voltage which includes also terms of high order. With the rf-deflector

set at its experimentally determined optimized phase ( $65^\circ$  for min. emittance growth) the measured displacement between the centers of the beams was 20 mm at a deflection voltage of 40 kV. This optimized phase determined by measuring the dependence of the emittance growth (deflection) on the relative rf-phase is shown in Fig. 7.

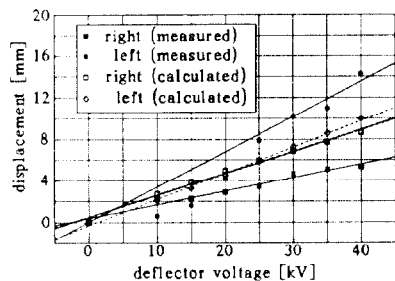


Fig. 5. The displacement as a function of the deflector voltage. The relative rf-phase  $\varphi$  is fixed to  $65^\circ$ .

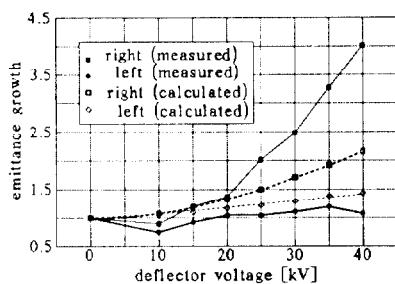


Fig. 6. The emittance growth as a function of the deflector voltage;  $\varphi = 65^\circ$ .

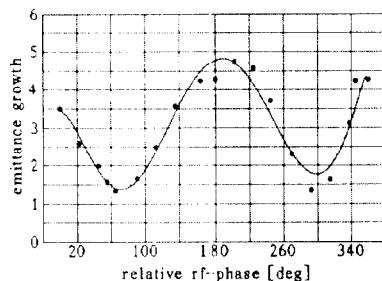


Fig. 7. The emittance growth as a function of the relative rf-phase, for a single bunch. The rf voltage has a constant value of 30 kV.

In Fig. 8, a comparison between the calculated and measured  $x, x'$ -emittance for two divided and parallel beams is shown. There are two effects which are predicted by the calculations and confirmed by the experiment: an offset in angle, which depends on the rf voltage (but independent on rf-phase) and moreover a rotation of the emittance, which is deflected to the right side. Both can be explained by the asymmetric field distribution. The value of the deflecting component of the rf-field is nearly independent on the direction of the deflection. But the longitudinal field component  $E_z(x, z)$ , as seen in Fig. 3b., shows a significant difference for a bunch deflected to the left or to the right side. This difference

explains all asymmetrically effects, which are shown in Fig. 5-9.

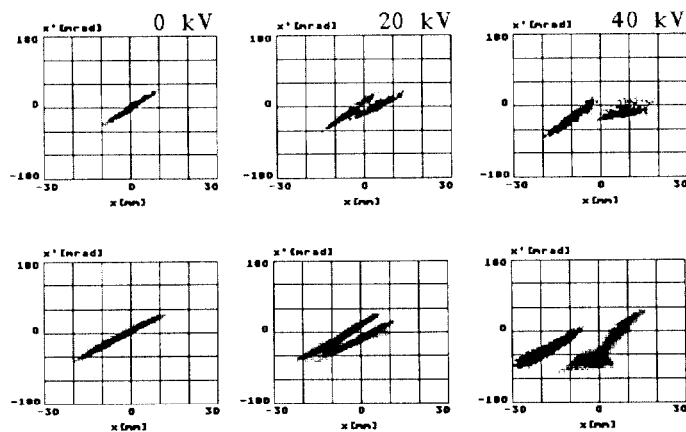


Fig. 8. The  $xx'$ -emittance as a function of the deflector voltage. The results of the simulations are shown on the top, those of the experiments on the bottom.

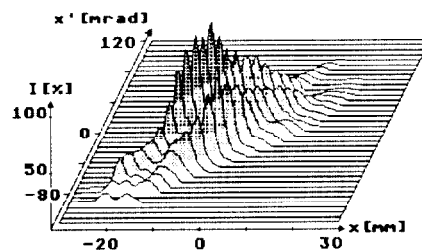


Fig. 9. The 3d  $xx'$ -emittance at a deflector voltage of 20 kV;  $\varphi = 65^\circ$ .

As a conclusion, the use of the defunnel experiments were successful. The dependence of beam deflection and horizontal emittance growth on deflection amplitude and relative rf-phase, as well as all asymmetries were explained by the simulations.

## VI. ACKNOWLEDGEMENTS

The authors thank all colleagues to their help, especially G. Hausen and I. Müller. All calculations were done at the HRZ/Frankfurt.

## VII. REFERENCES

- [1] T.P. Wangler et. al., Linac, LA-12004-C (1990), 548.
- [2] R.H. Stokes, G.N. Minerbo, IEEE, Vol. NS-32 No.5, (1985).
- [3] K. Bongardt, D. Sanitz, HMF, GSI 82-8 (1982), 224.
- [4] J.F. Stovall et. al., NIM A278 (1989).
- [5] K.F. Johnson et. al., Linac, LA-12004-C (1990), 701.
- [6] W.B. Herrmannsfeldt, SLAC Rep. 166, (1973).
- [7] W. Sinz, thesis, Univ. Frankfurt, (1986).
- [8] K. Langbein, EPAC, Rome, (1988), 1228.
- [9] P. Leipe, Univ. Frankfurt, thesis, (1989).
- [10] A. Müller Rentz, Univ. Frankfurt, dipl. thes., (1986).
- [11] G. Riehl, Univ. Frankfurt, thesis, (in prep.).
- [12] W. Barth, GSI Darmstadt, rep. 91-1, in print, (1991).